

Graded Interlocks for Iontronic Pressure Sensors with High Sensitivity and High Linearity over a Broad Range

Ningning Bai, Liu Wang, Yiheng Xue, Yan Wang, Xingyu Hou, Gang Li, Yuan Zhang, Minkun Cai, Lingyu Zhao, Fangyi Guan, Xueyong Wei, and Chuan Fei Guo*



Cite This: *ACS Nano* 2022, 16, 4338–4347



Read Online

ACCESS |



Metrics & More



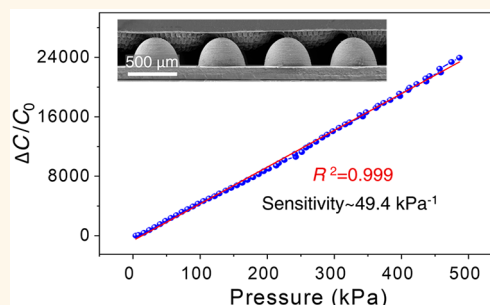
Article Recommendations



Supporting Information

ABSTRACT: Flexible pressure sensors that have high sensitivity, high linearity, and a wide pressure-response range are highly desired in applications of robotic sensation and human health monitoring. The challenge comes from the incompressibility of soft materials and the stiffening of microstructures in the device interfaces that lead to gradually saturated response. Therefore, the signal is nonlinear and pressure-response range is limited. Here, we show an iontronic flexible pressure sensor that can achieve high sensitivity (49.1 kPa^{-1}), linear response ($R^2 > 0.995$) over a broad pressure range (up to 485 kPa) enabled by graded interlocks of an array of hemispheres with fine pillars in the ionic layer. The high linearity comes from the fact that the pillar deformation can compensate for the effect of structural stiffening. The response-relaxation time of the sensor is $< 5 \text{ ms}$, allowing the device to detect vibration signals with frequencies up to 200 Hz. Our sensor has been used to recognize objects with different weights based on machine learning during the gripper grasping tasks. This work provides a strategy to make flexible pressure sensors that have combined performances of high sensitivity, high linearity, and wide pressure-response range.

KEYWORDS: *graded interlocks, iontronic interface, compressibility, linearity, pressure range*



INTRODUCTION

With the development of intelligent robots and wearable healthcare technologies,^{1–6} flexible pressure sensors have called for increasingly improved performances. An ideal flexible pressure sensor should exhibit combined properties of high sensitivity, high linearity, and a wide pressure-response range.⁷ The high sensitivity allows the sensor to detect subtle mechanical stimuli; the linear signal can result in a simplified circuit used to process the signal and more accurate detection of the stimuli; and sensors with a wide pressure-response range can have much more application scenarios than that with a narrow range. For example, the emerging soft-rigid hybrid robots can achieve a much broader loading range than conventional soft robots, but they need flexible pressure sensors that have high sensitivity over a wide pressure-response range to serve for them to achieve sensing function and accurate feedback.⁸ Furthermore, in wearable virtual reality devices,⁹ pressure sensors with high sensitivity and highly linear signals provide a more realistic tactile feeling.

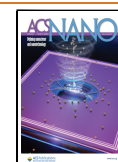
Capacitive-type flexible pressure sensors can serve as a preferred selection of sensing devices in tactile perception

systems, because of their simple device structure, stable signal, and low energy consumption.^{10,11} A flexible capacitive sensor often has a trilayered structure of two electrodes sandwiching a soft dielectric. The capacitance is expressed as $C \approx \epsilon A/d$, where ϵ is the permittivity, A the contact area between the electrode and the dielectric, and d the distance between the two electrodes.¹² Because soft dielectric is incompressible (volume does not change upon loading), the capacitance can have limited change and, thus, sensitivity is low. The introduction of microstructures such as microcones,^{13,14} micropillars,^{15,16} micropillars,^{17,18} can improve the sensitivity of the sensors by improving the compressibility of the soft dielectric. Such microstructures, on the other hand, are susceptible to signal saturation, because of structural stiffening

Received: November 28, 2021

Accepted: January 28, 2022

Published: March 2, 2022



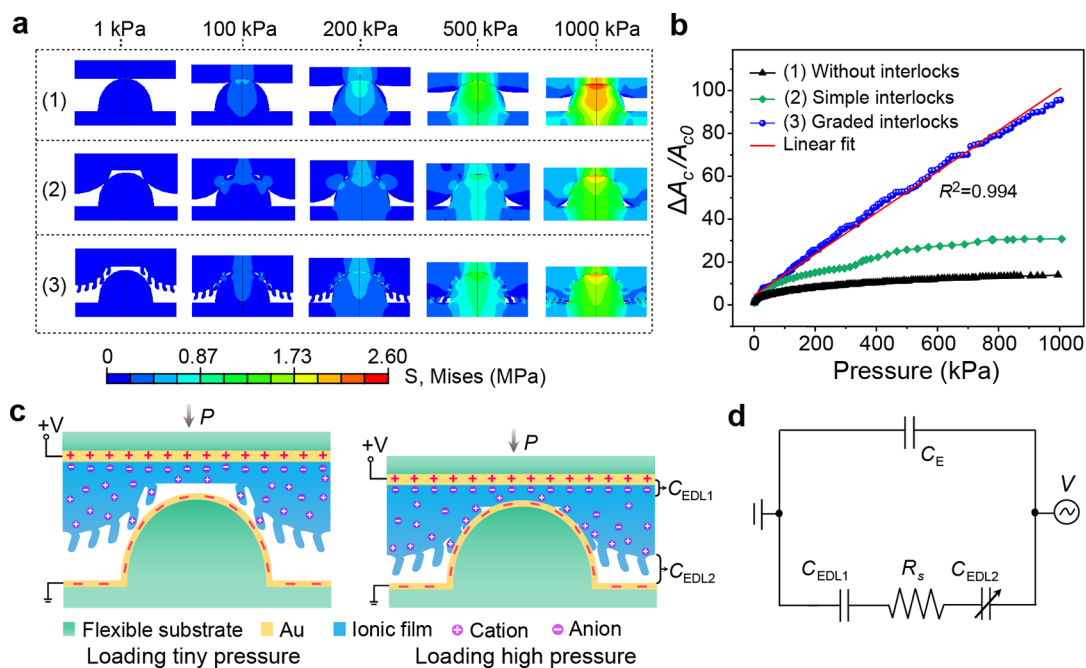


Figure 1. Compressibility of the graded interlocks and its sensing principle. (a) Compressibility and stress distribution of the three interfacial configurations under pressures up to 1 MPa: dome-plane interfaces without interlocks, simple interlocks, and graded interlocks. (b) Normalized change in contact area change for the three configurations under pressures over 1 MPa. (c) Schematic for the sensing mechanism of the iontronic pressure. (d) Simplified equivalent circuit diagram of the iontronic pressure sensor.

that leads to a stronger resistance to increasing load. As a result, the sensors show poor performances, in terms of signal linearity and sensing range. Higher linearity in capacitive sensors has been achieved by using a percolative elastomeric composite of which the mechanical saturation is compensated by the increased permittivity,¹⁹ or by elaborately designing foam structures as the dielectric layer.^{20–22} However, those aforementioned sensors present a low sensitivity of 0.0046 and 0.00049 kPa^{-1} , respectively, as a result of the poor compressibility of the dielectric layer. Iontronic sensors are a class of devices that exhibit extremely high sensitivity; these have been developed in recent years.^{23–27} Different from conventional capacitive pressure sensors, iontronic sensors employ an ionic film to replace the dielectric layer. The high sensitivity lies in the electric double layer (EDL) formed at the electrode/ionic film interface, which has a separation of ~ 1 nm for the positive and negative charges. Signal enhancement by a few orders of magnitude can be achieved because the charge separation is much smaller than that of conventional capacitive sensors (mostly 10–100 μm).²⁶ For example, a graded intrafillable architecture-based iontronic pressure sensor with a high sensitivity ($>200 \text{ kPa}^{-1}$) up to 360 kPa and micropillar-based iontronic pressure sensor with a high sensitivity (33.16 kPa^{-1}) over a pressure range of 12–176 kPa have been developed by Guo and co-workers.^{28,29} Recently, Xiao et al. reported a multilayer double-sided microstructured iontronic pressure sensor that achieves a sensitivity of 10 kPa^{-1} over a pressure up to 2 MPa.³⁰ Despite the high sensitivity, existing iontronic sensors either do not have linear pressure response,²⁸ or suffer from a convoluted fabrication process.³⁰ A feature of the iontronic sensor is that the capacitance is simply determined by the interfacial contact area A_c between the electrode and the ionic film, following $C \propto A_c$. This feature can simplify the design of sensors, since there is only a single parameter to be considered to design a structure for which the

interfacial contact area increases linearly with pressure over a wide range.

Here, we report a 3D-printed flexible iontronic pressure sensor with high sensitivity (49.1 kPa^{-1}) and high linearity ($R^2 \approx 0.998$) over a wide linear working range up to 485 kPa. The combined high performances are enabled by the iontronic interface of graded interlocks that improve the compressibility by structural complementation and compensate the structural stiffening by the deformation of dense microscale pillars. The graded structures also lead to an ultrafast response-relaxation time of <5 ms and thus the sensor can detect vibration frequencies up to 200 Hz. We further applied the sensor to robotic gripping tasks to recognize the weights of the grasped objects based on machine learning, exhibiting recognition accuracies of $>88\%$. This work provides a strategy to fabricate flexible pressure sensors with combined properties of high sensitivity, high linearity, and a wide pressure-response range for robotic manipulations.

RESULTS AND DISCUSSION

Design Principle of the Graded Interlocks and Sensing Mechanism of the Device. The compressibility of microstructures at the interface of sensors determines their sensing properties. It has been proven that the proper design of such microstructures can regulate the sensitivity and pressure-response range of the devices.^{28,31,32} Here, we introduce a nanoscale iontronic interface in sensors with submillimeter interlocked structures that show high compressibility and can delocalize stresses to avoid signal saturation or nonlinearity, and the stresses can further be uniformized by introducing smaller-scale slender structures that fill in the gaps of the interlocks. The nanoscale iontronic interface consists of an ionic layer of poly(vinyl alcohol) (PVA) and phosphoric acid (H_3PO_4), and an electrode of gold-plated flexible epoxy resin. The PVA/ H_3PO_4 surface has an array of submillimeter

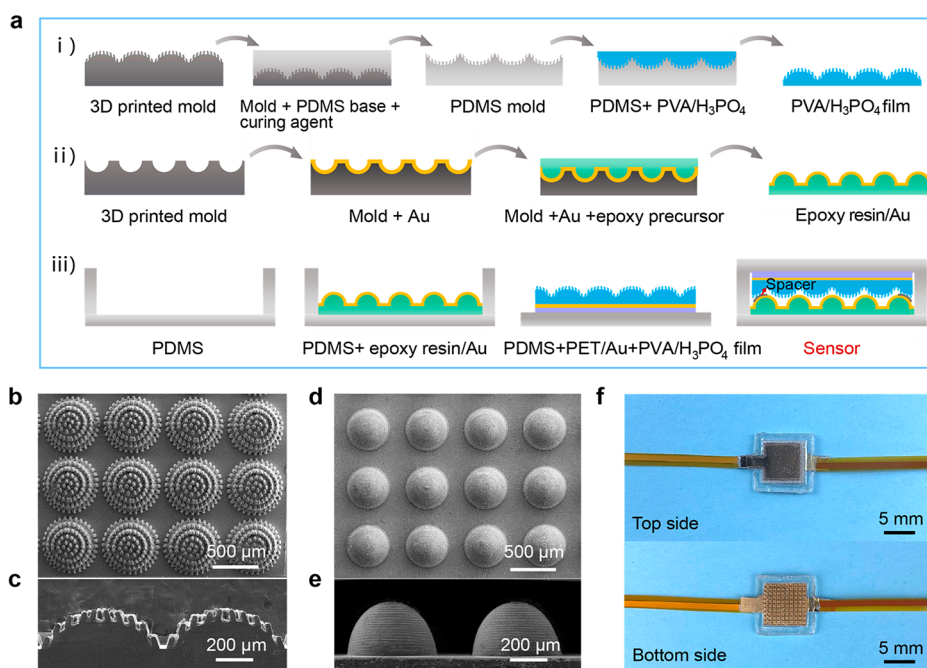


Figure 2. Preparation of the graded interlock-based iontronic pressure sensor. (a) Schematic of the preparation of the iontronic pressure sensor. (b, c) SEM images of the PVA/H₃PO₄ film from (b) top view and (c) side cross section view. (d, e) SEM images of the epoxy resin/Au electrode from (d) top view and (e) side view. (f) Top and bottom photographs of the pressure sensor.

semiellipsoids grown with micropillars, while the electrode has large microdomes only and is placed opposite to the ionic layer to form interlocks. An EDL is formed at the iontronic interface when the ionic layer makes contact with the electrode, and its capacitance is in direct proportion to the interfacial contact area. Therefore, in iontronic sensors, the regulation of linearity is simple—only a single parameter (A_c) must be considered.

We studied three dome-based configurations of iontronic interface with different levels of compressibility determined using finite element analysis (FEA), as shown in Figure 1a: (1) domes placed against a flat surface without forming interlocks; (2) simple interlocks consisting of top and bottom domes; and (3) graded interlocks of semiellipsoidal structure with secondary micropillars, which are placed against smooth domes. Because A_c is related to the compressibility, we extracted the change in contact area (ΔA_c) from the FEA result to determine the response to the pressure of the iontronic interfaces. The first configuration (and many other configurations alike) has been commonly used in flexible pressure sensors,^{27,28} but the gaps between the domes and the flat surface can hardly be occupied. As a result, the compressibility of the interface is poor, and corresponding $\Delta A_c/A_{c0}$ (A_{c0} is the initial contact area), as a function of pressure, is small (Figure 1b). Such gaps can be largely filled using interlocks, and we show that, in the second configuration (simple interlocks), the compressibility is significantly improved and $\Delta A_c/A_{c0}$ becomes more than one time larger. However, there are still gaps in such interlocks that cannot be filled up, and saturation and nonlinearity of the $\Delta A_c/A_{c0}-P$ plot still occur. In the third configuration, the gaps between the domes can be further filled by the slender micropillars, and $\Delta A_c/A_{c0}$ is remarkably increased and determined to have high signal linearity with a high correlation coefficient ($R^2 = 0.994$).

The micropillars play important roles. On one hand, they improve the compressibility, uniformize the stress distribution, and contribute to the high linearity of the $\Delta A_c/A_{c0}-P$ plot. As

the pressure increases, the micropillars contact the electrode, buckle, and gradually fill the gaps between the structures of the ionic layer and the electrode. It is the collective behavior of the pillars that significantly uniformizes the stresses at the interface, thereby relieving the structure stiffening that otherwise causes signal saturation of the sensors. The stress distribution is much more nonuniform if without introducing such dense micropillars on the submillimeter domes. On the other hand, the micropillars minimize the initial contact area A_{c0} of the iontronic interface and improve the sensitivity of the device. Because the sensitivity of iontronic pressure sensors is in direct proportion to the normalized change in contact area ($\Delta A_c/A_{c0}$), a smaller A_{c0} can result in improved sensitivity.

Here, the graded interlocked EDL interface has a variable contact area that is determined by the applied pressure, as shown in Figure 1c. Note that there are two EDL capacitors formed at the flat interface (denoted as C_{EDL1}) and the microstructured interface (denoted as C_{EDL2}), respectively. The two capacitors are connected in series with a bulk resistance (R_s) and in parallel with a coupling capacitance C_E generated by the two electrodes (Figure 1d). The measured capacitance can be defined as $C = C_E + 1/[(1/C_{EDL1}) + (1/C_{EDL2})]$. Here, C_{EDL1} has a large value and is constant because of its full contact; C_{EDL2} is sensitively changed upon loading; and C_E is far smaller, compared with the EDL capacitance, such that it can be neglected. Notably, the microstructure deformation at the iontronic interface is unsaturated within 1 MPa. Therefore, when the applied pressure is not high, C_{EDL2} is much smaller than C_{EDL1} , and the measured capacitance (C) is approximately equal to C_{EDL2} , which is determined by the contact area of the iontronic interface. Since our FEA simulation indicates a linear A_c-P relationship of the graded interlocks, sensors applying such structures are expected to show linear responses to applied pressure. Overall, the graded interlocks allow for greater compressibility of the structure, resulting in linear variation in contact area with increasing pressure. The

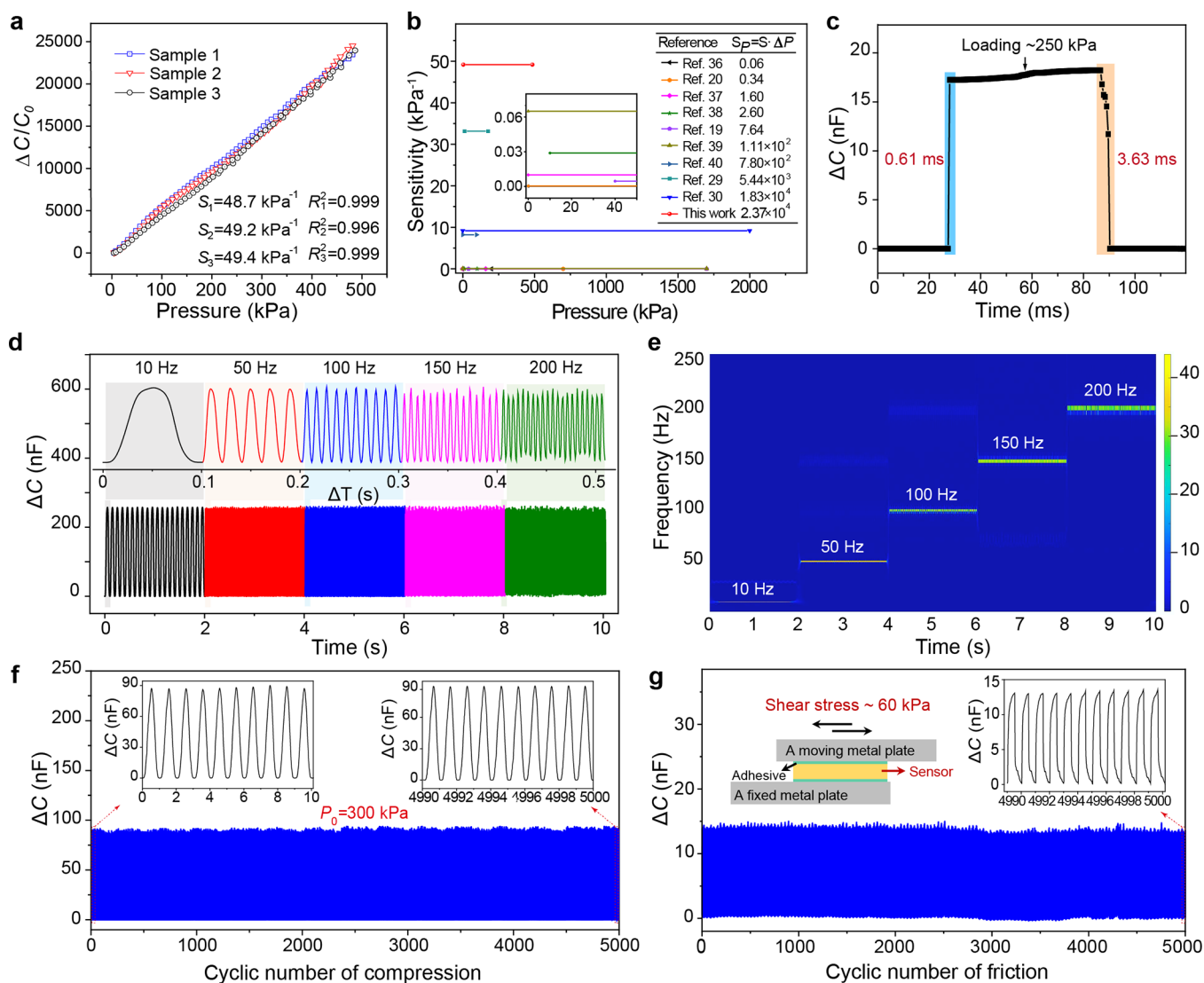


Figure 3. Sensing properties of the graded interlocked structure-based iontronic pressure sensor. (a) Normalized change in capacitance as a function of pressure up to 485 kPa. (b) Comparison of our iontronic sensor with other capacitive sensors with high linearity in terms of sensitivity, linear sensing range, and S_p . (c) Response and relaxation time when loading a pressure of ~ 250 kPa and release. (d) Time-dependent variation of capacitance at different vibration frequencies. (e) Wavelet transform signal of the different vibration signals shown in panel (d). (f) Compression-release test over 5000 cycles under a high pressure of 300 kPa. (g) Friction stability of the device over 5000 cycles at a peak shear stress of ~ 60 kPa.

structural design synergizes with the signal enhancement provided by the nanoscale iontronic interface to achieve a high sensitivity, linear response and wide sensing range for the sensor.

Preparation of the Graded Interlocked Structure-Based Iontronic Pressure Sensor. The fabrication of the sensor involves three steps: the fabrication of the structured ionic film, the fabrication of the structured electrode, and device encapsulation, as shown in Figure 2a. For the fabrication of the structured ionic film and the structured electrode, we first 3D-printed resinous structures using the models in the FEA simulation, serving as the molds to further make the ionic layer and the electrode. The dimensions (height, width, pitch, etc.) of the graded interlocking structures prepared here are determined by the structural design based on FEA simulation, as well as the limitations of the 3D printer.

Figures 2b–e show the top view and side view scanning electron microscopy (SEM) images of the PVA/H₃PO₄ film

(Figures 2b and 2c) and that of the epoxy resin/Au electrode (Figures 2d and 2e). The PVA/H₃PO₄ layer has an array of uniform semiellipsoidal structures (width = 580 μ m, height = 165 μ m, pitch = 75 μ m) with 97 upright micropillars (diameter = 28 μ m, height = 70 μ m) on top; and the flexible electrode of epoxy resin/Au has uniform microdomes with a pitch of 190 μ m and a slightly larger aspect ratio (width = 290 μ m, height = 480 μ m), which can form interlocks with the ionic film microstructures. The sensor was encapsulated using flexible epoxy resin/Au with domed structure as the bottom electrode, microstructured PVA/H₃PO₄ film as the active layer, and 6- μ m-thick double-sided tape as a spacer, warranting the same initial contact state between the electrode and ionic layer in different sensors such that the initial capacitance is within several picofarads, because of the air gap, and a gold-plated polyethylene terephthalate (PET) film as the top electrode. Here, two pieces of copper-plated polyimide strips were adhered to the top and bottom electrodes using silver paste to

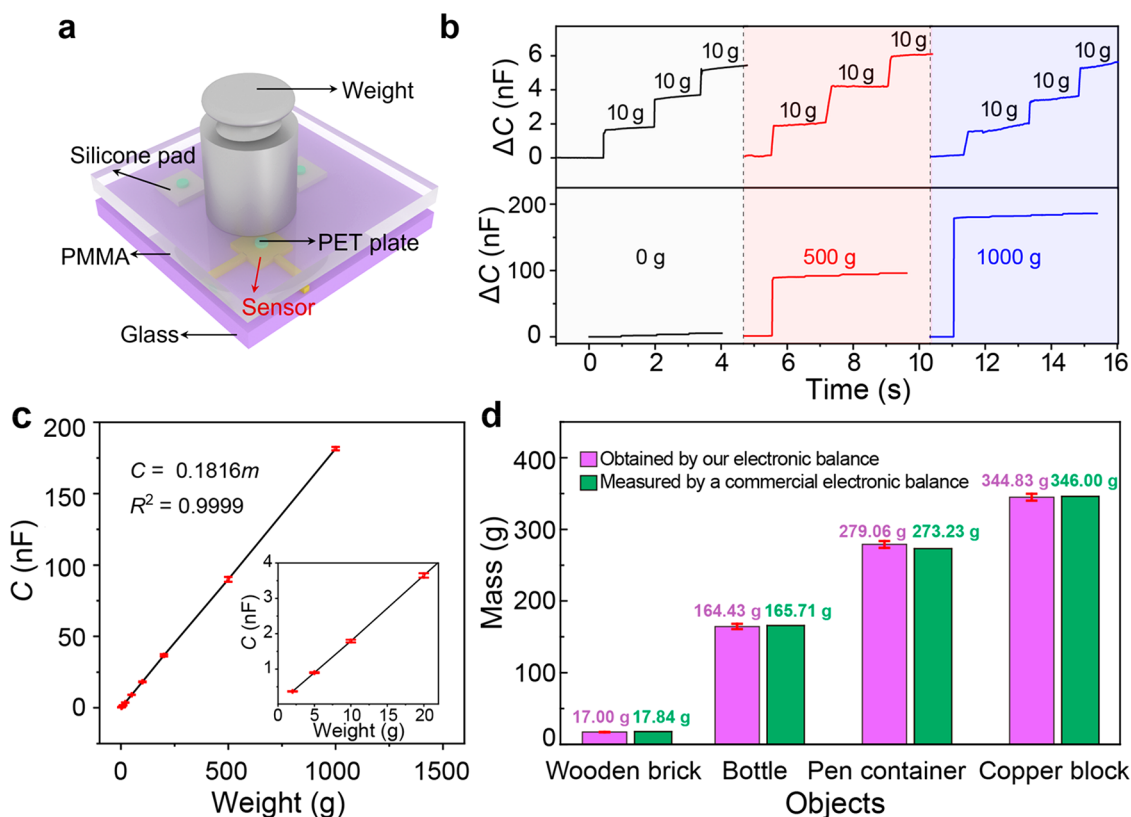


Figure 4. Linear response of the pressure sensor. (a) Schematic diagram of the simple electronic balance using the sensor. (b) Changes in capacitance when loading three 10 g weights in sequence on the electronic balance under different basic weights of 0, 500, and 1000 g. (c) Fitted curve for capacitance versus mass when loading standard weights of 2, 5, 10, 20, 50, 100, 200, 500, and 1000 g. (d) Comparison of masses for the objects measured by our electronic balance and a commercial electronic balance.

connect to an LCR meter for capacitance measurement. Later, polydimethylsiloxane (PDMS) films were used as the packaging material to encapsulate the four layers as an entirety. All surfaces except for that of the microstructured iontronic interface were plasma-treated to introduce chemical bonds between the layers.³³ Figure 2f shows two photographs of the flexible iontronic pressure sensor, and the flat top electrode and the structured bottom electrode can be observed through the transparent PDMS layer. The bending test at a bending radius (r) of ~ 3 mm reflects the desired flexibility and sensitive response of the pressure sensor to bends (see Figure S1 in the Supporting Information), which allows it to be used for bending-related applications, such as motion monitoring of wrist joint bending and knee joint bending.

The microstructured electrode is required to have a low and stable resistance. In this work, we used epoxy resin as the electrode substrate, because it is a metal binder that forms high bonding strength with metals.^{34,35} The strong adhesion leads to the high stability of the electrode: after the electrode is bent under high curvature or twisted for several times, its resistance remains within 10Ω , proving that the electrode is highly flexible and stable (Figure S2 in the Supporting Information). After cyclic compression release over 20 000 cycles at a peak pressure of 300 kPa (Figure S3 in the Supporting Information), or after a friction test over 20 000 cycles at a maximum pressure of 100 kPa (Figure S4 in the Supporting Information), little drift in resistance and no failure of the microstructures was observed. The high stability of the electrode enables the sensor to work stably under strains.

Sensing Properties of the Pressure Sensor. Sensitivity, linearity of the signal, and sensing range are the key parameters of the sensor in this study. The sensitivity of a pressure sensor is defined as $S = \delta(\Delta C/C_0)/\delta P$, where C_0 is the initial capacitance before loading, and ΔC refers to the variation of the capacitance when imposed to an applied pressure P . Before pressure is applied, the microstructured electrode is not in contact with the ionic layer (i.e., an air gap in between) because of the presence of the spacer, thus providing a low C_0 (~ 5.9 pF). When the pressure is less than 4 kPa, only the air gap between the electrode and the ionic layer is compressed, which leads to a tiny change of the capacitance (Figure S5a in the Supporting Information). At the pressure of 4 kPa, the electrode begins to contact the ionic layer. Figure 3a presents the normalized change in capacitance with pressure from 4 kPa to 485 kPa of three different devices. At this stage, the capacitance increases sharply with pressure (Figure S5b in the Supporting Information) and changes with test frequency because of the existence of EDL (Figure S6 in the Supporting Information), which is an intrinsic characteristic of iontronic sensors. The three sensors all exhibit linear response with close sensitivity values ($S_1 = 48.7 \text{ kPa}^{-1}$, $S_2 = 49.2 \text{ kPa}^{-1}$ and $S_3 = 49.4 \text{ kPa}^{-1}$ for the three devices) over a wide sensing range up to 485 kPa. In addition, the average correlation coefficient of the $\Delta C/C_0$ - P curves is as high as 0.998 ($R_1^2 = 0.999$, $R_2^2 = 0.996$, and $R_3^2 = 0.999$ for the three samples). The results agree well with our design based on the graded interlocks of an iontronic interface.

Here, we define a parameter that we call the linear sensing factor (S_p) that can reflect both sensitivity and linear sensing

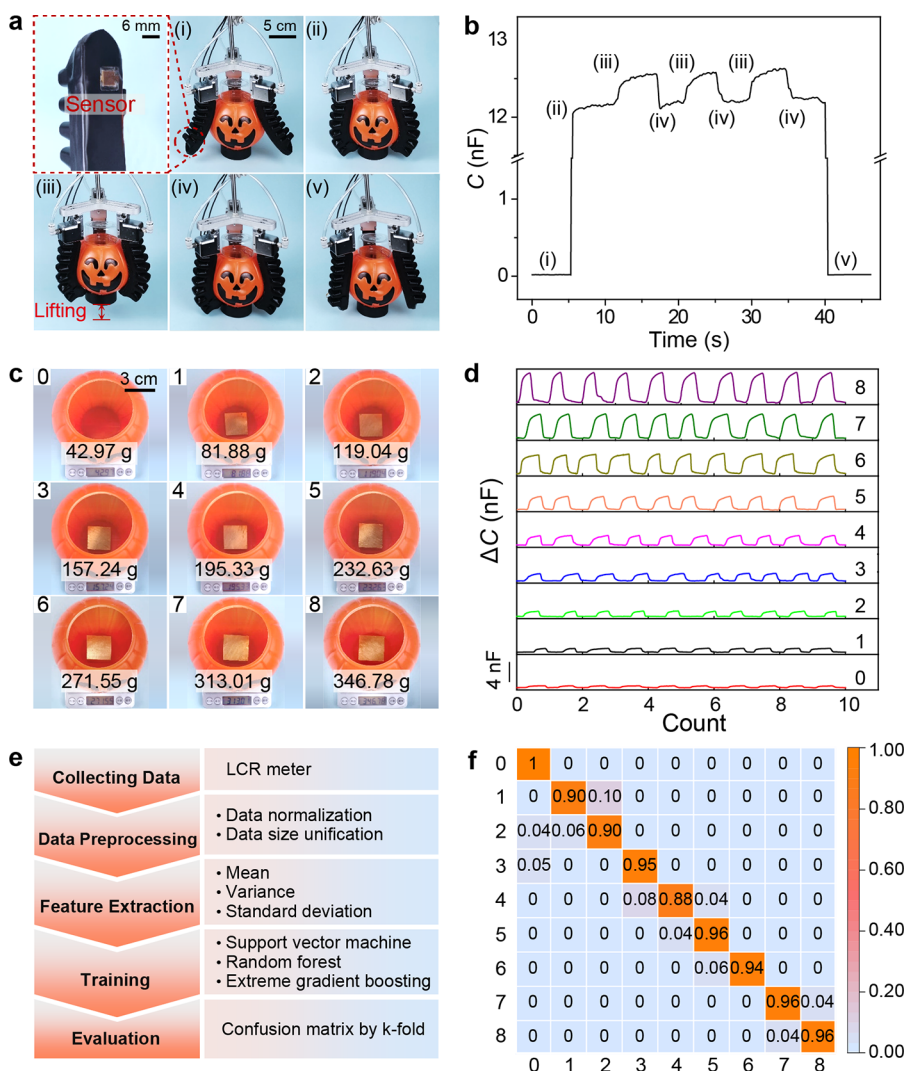


Figure 5. Sensing in gripping task and identification of weight based on machine learning. (a) The process of grasping a container using a pneumatic gripper integrated with our sensor. (b) Capacitance changes at different stages of the gripping process. (c) Photograph of the container with the different masses of copper blocks. (d) Output signals corresponding to gripping the container with different mass of copper blocks. (e) A simplified diagram for implementing machine learning. (f) Confusion matrix to weight distinguish derived from machine learning with 42 sets of data for each category. The x -axis of the confusion matrix is the predicted values and the y -axis is the actual values.

range (ΔP), $S_p = S \cdot \Delta P$. Generally, both high sensitivity and a broad linear sensing range are required to achieve a large S_p . Figure 3b shows the comparison of both sensitivity and linear sensing range of our sensor with existing capacitive sensors that have linear signals,^{19,20,29,30,36–40} and the corresponding S_p values are also listed in the inset and Table S1 in the Supporting Information. We can see that most reported flexible capacitive sensors have a small S_p values, because of either low sensitivity or narrow linear sensing range. For example, Wu et al. reported a sensor with an impressive linear sensing range of 40–1700 kPa,¹⁹ while its sensitivity is only 0.0046 kPa⁻¹, and thus the sensor has a low S_p value of 7.64. Iontronic pressure sensors can provide improved sensitivity. Recently, Xiao et al. reported an iontronic sensor with 12 layers of double-sided microstructured ionic film, exhibiting a higher sensitivity of 9.17 kPa⁻¹, a wide linear sensing range of 2000 kPa,³⁰ and a large S_p value of 1.83×10^4 . However, the many-layered structures are thick, and the process to make the sensor is complicated. By contrast, our sensor has a better linear sensing

capability ($S_p = 2.37 \times 10^4$), together with a much simpler device structure.

The response speed is another important parameter of a pressure sensor, and has been widely used to assess its dynamic response. Introducing microstructure can accelerate the response speed of sensors due to that the microstructures can quickly store and release energy for elastic recovery.¹¹ Here, the graded interlocks exhibit two scales of structures: the submillimeter domes, and secondary micropillars on the submillimeter ellipsoids, which can further effectively reduce response-relaxation time. When subjected to a pressure of ~ 250 kPa, our sensor reacts rapidly to the stimulus with a response time of 0.61 ms and a relaxation time of 3.63 ms (Figure 3c), which are much shorter than that of the human skin and most flexible pressure sensors reported previously.^{1,14,24,28–30} With the quick feedback time of 4.24 ms, the sum of the response time and the relaxation time, the graded interlock-based iontronic sensor can detect vibration signals of a broad range of frequencies with the highest

vibration frequency up to 200 Hz, as shown in Figure 3d, and Figure 3e is the corresponding wavelet transform results which further show the variation of the frequencies with time generated by the vibrations. The rapid response and relaxation speed allow the device to identify dynamic signals with high frequencies.

Mechanical durability is of great importance to the application of flexible pressure sensors. Repeated compression-release to a pressure of 300 kPa over 5000 cycles was conducted, and the sensor shows no significant drift or fluctuation throughout the cyclic test (Figure 3f). The negligible hysteresis (Figure S7 in the Supporting Information) during the loading/unloading test indicated that the pressure sensor can respond reversibly. The sensor is further firmly adhered to two metal plates to characterize its shear stability. Figure 3g confirms the high stability of the device when subjected to frictions with a peak shear stress of 60 kPa. In addition, the device is encapsulated to block the contact of the ionic film with external moisture because the PVA/H₃PO₄ layer is humidity-sensitive, and the seal can effectively eliminate the signal drift caused by external humidity change (Figure S8 in the Supporting Information).

Linear Response of the Pressure Sensor. We further demonstrate that the linear response is potentially useful in real applications. As shown in Figure 4a, the sensor was used to manufacture a simple electronic balance. We examined the signal changes when loading three weights (10 g each) in sequence on the electronic balance under different basic weights of 0, 500, and 1000 g (the experimental setup; see Figures S9a and S9b in the Supporting Information). As shown in Figure 4b, when the weight increases linearly, the electronic balance can output a linearly changed signal. In order to systematically and reliably determine the relationship between the output capacitance signal and the loaded weight mass, the electronic balance was used to test different standard weights (i.e., 2, 5, 10, 20, 50, 100, 200, 500, and 1000 g) and each was tested three times. The relationship between the output capacitance (C) with the mass (m) of the added weight is shown in Figure 4c. Based on a linear fit with a high R^2 of 0.9999 to the output, we achieve a C value of $0.1816m$. Next, the electronic balance was applied to detect the undetermined mass of a wooden brick, a bottle, a pen container, and a copper block, with each object being tested three times and the corresponding output values were recorded. As shown in Figure 4d, the mass of the objects tested using our electronic balance is very close to those measured using a commercial electronic balance (Figure S10 in the Supporting Information), with deviations of 4.7%, 0.77%, -2.13%, and 0.34% to the linearly fitted values, respectively. Such small deviations indicate that mechanosensing using our sensor is quite simple—nonlinear calibration is no longer required.

Sensing in Gripping Task and Identification of Weight Based on Machine Learning. An important application of flexible pressure sensors is to bring the haptic capability to robots, allowing them to interact with the outside world like human beings. For example, sensors equipped on robots can provide tactile information to ensure more precise manipulations. Here, our sensor was integrated on a pneumatic gripper that was used to grasp a container, and the capacitive signal during the manipulation was recorded. In Figure 5a, we show that the gripping process contains five stages: (i) precontact phase; (ii) grasp without lifting the object up; (iii) lifting; (iv) placing the object back; and (v) release of the

object. Figure 5b shows the signal corresponding to the gripping process, with the third and fourth stages repeated three times. In the precontact phase, the sensor exhibits a low initial capacitance C_0 . As soon as the soft robot grips the container, the signal rises up rapidly and finally remains at a fixed value determined by the applied pressure that drives the robot. In stage iii, the signal magnitude increases as the gripper lifts up the container and decreases in stage iv, in which the container is landed back. The signal amplitude returns to C_0 in stage v due to the separation of the gripper and the container.

Afterward, we tried to use the soft robot with our sensor to identify the mass of objects added into the container. First, copper blocks with different mass were dropped into the container (Figure 5c). Notably, the process of lifting the container from the table and placing it back was conducted several times to verify the repeatability of the sensing signals, and Figure 5d shows that the output signals can well reflect the mass of the added weights. The output magnitude enhances as the mass of the added copper block increases, making it possible to distinguish the weight of the grasped object during the grasping process.

Machine learning in combination with pressure sensing has proven to be effective to determine the weight of objects.^{41,42} Here, machine learning is used to analyze the signals captured by our sensor, which can further be used to realize precise feedback. Figure 5e is a simplified diagram for implementing machine learning. We adopted the K-Fold cross-validation method to recycle the data and divide the data into n parts, using one of the parts as the test set without duplicates and others as the training set. Each category was tested for 10 times, and 10 accuracy values were obtained. Next, the average value of the accuracy was taken as the final output of the confusion matrix shown in Figure 5f. The results show that the gripper integrated with our device has recognition accuracies of >88% for all these added objects with different weights. Therefore, our sensor is expected to be used to achieve precise haptic sensations for robots with the aid of machine learning.

CONCLUSIONS

In this study, graded interlock-based iontronic flexible pressure sensors that exhibit high sensitivity and highly linear response over a wide pressure range have been fabricated and applied to the haptic sensation of soft robots. The combined high performances stem from the high signal magnitude provided by the nanoscale iontronic interface as well as the compensation of the structural stiffening of the microscale pillars. The sensor also exhibits fast response-relaxation speed and can detect vibration with frequencies up to 200 Hz, providing the possibility to detect fluctuating and dynamic loads. We have developed a simple electronic balance based on our sensor that can accurately measure the mass of objects. The integration of our sensor on a soft gripper enables the robot to recognize the mass of grasped objects by machine learning with a recognition accuracy of >88%, exhibiting potential applications in robotic haptics.

MATERIALS AND METHODS

Preparation of the PVA/H₃PO₄ Ionic Film with the Graded Semiellipsoidal Structure. We adopted a printed template to prepare the ionic film with hemispheric graded structure. The mold with micropillars distributed on semiellipsoids was made using a high-precision printing equipment (nanoArch S130, BMF Precision Tech, Inc.) based on projection micro stereolithography. The first mold was

obtained by casting the mixture of PDMS base and curing agent (Sylgard 184, Dow Corning Co., Ltd.) in a weight ratio of 5:1, and curing at 80 °C for 30 min. Our previously reported hybrid system of PVA (Mw \approx 145 000, from Aladdin Industrial Corporation) and H₃PO₄ (AR, \geq 85%, Shanghai Macklin Biochemical Co., Ltd.) was used as the ionic film. First, 1 g of PVA was dissolved in 9 g of deionized water and stirred for 2 h at 90 °C until it is completely dissolved. After the solution was cooled to 50 °C, 0.8 mL of H₃PO₄ was added to the PVA solution and stirred for 1 h. Next, the PVA/H₃PO₄ solution was cast on the PDMS template and cured at 24 °C for 24 h. Finally, a PVA/H₃PO₄ film with a thickness of \sim 330 μ m was peeled off and then cut into squares with a side length of 8 mm for later use.

Preparation of Flexible Electrodes. The planar PET/Au film, as the top electrode, was prepared by depositing 200-nm-thick gold on a PET film (HD, DuPont) with a thickness of 50 μ m using ion sputtering (MC1000, Hitachi High-Tech Corporation) at a current of 25 mA for 300 s. The flexible epoxy resin/Au film with domes that have a thickness of \sim 360 μ m was used as the bottom electrode, which was obtained by the following steps.

- (1) Designing a reverse domed structure and printing the mold using high-precision three-dimensional (3D) printing.
- (2) The gold film was deposited on the mold surface at a current of 25 mA for 300 s using the ion sputter (MC1000, Hitachi High-Tech Corporation).
- (3) Difunctional bisphenol A based epoxy prepolymer (EPIKOTE Resin 828, XEXION) and the oligomeric polyamine curing agent (EPIKURE Curing Agent 3164, XEXION) were dissolved in acetone at a weight ratio of 5:5:1 (epoxy prepolymer, curing agent, and acetone, respectively).
- (4) The mixed solution was coated on the gold-plated mold and spun at the speed of 1000 rad/s for 1 min using a spin coater (WS-650MZ, MYCRO).
- (5) The mixed solution on the mold was cured at 24 °C for 5 h to form an incompletely cured state and then continued to cure completely at 80 °C for 2 h.
- (6) The flexible epoxy resin/Au electrode with domes was peeled off and then cut into squares with side length of 7 mm for later use.

Note that, here, two copper-plated polyimide strips were adhered severally to each of the top and bottom electrodes using silver paste (FS05001-AB, SPI Corporation) for connection to the test device.

Preparation of the Graded Interlocked Structure-Based Iontronic Pressure Sensor. The sensor consists of six layers, from bottom to top, followed by bottom packaging material, a bottom electrode, a spacer, an ionic film, a top electrode, and top packaging materials. Both the non-gold-plated sides of the PET/Au film and flexible epoxy/Au electrode with domed structure were treated by plasma and then bonded on the surface of the top and bottom PDMS layers after plasma treatment, respectively. Next, a piece of 6- μ m-thick double-sided PET tape (PET-6, Dongguan Innovation Electronic Materials Co., Ltd., China) as a spacer was adhered to the flexible epoxy/Au electrode with domed structure, and the PVA/H₃PO₄ film was sandwiched between two electrodes later. Finally, the PDMS of the top and bottom layers were glued together by silicone rubber adhesive (Sil-Poxy, Smooth-On, Inc.).

Finite Element Analysis. FEA was performed using commercial package Abaqus 2017. Two-dimensional model was built for simplicity. The microstructured ionic film and epoxy resin/Au electrode are modeled with incompressible Neo-hookean materials with Young's moduli of 2 MPa (Figure S11 in the Supporting Information) and 20 MPa (Figure S12 in the Supporting Information), respectively. Frictionless contact without penetration is assumed. The total contact area is recorded as the pressure increases up to 1 MPa. The initial contact area A_{c0} is determined at the pressure of 4 kPa. Detailed stress distribution under various pressures is shown in Figure 1a.

Characterization and Measurements. The morphology of ionic film and electrode were probed using field-emission scanning

electron microscopy (TESCAN MIRA3) operated at 5 kV. All output capacitances were collected using a precision LCR meter (Model E4980AL, KEYSIGHT) at a test frequency of 1 kHz, except for the capacitance in response time measurements for which the data were collected using a high-speed LCR digital bridge (TH2840B, TONGHUI) working at a test frequency of 10 kHz. The resistance of the electrode was tested using a digital multimeter (Model 2100, KEYSIGHT). A multifunctional tension/compression testing system (Model XLD-20E, Jingkong Mechanical Testing Co., Ltd.) was employed to exert and record applied force. The vibration signal applied to the device in Figure 3d was generated using a vibration generator (Model BL-ZDQ-2185, Hangzhou Peilin Instrument Co.). In the friction test (Figure 3g), the flexible pressure sensor is glued to two metal plates by the silicone rubber adhesive to ensure that the sensor is fixed firmly without any slip over the cyclic test. One metal plate was fixed, and the other one is moved back and forth at a distance of 0.5 mm by traction of a multifunctional tension/compression testing machine during the test. The grasping task (Figure 5) is performed using a pneumatic gripper (FM-A4 V4/LS1[AS]-A8, Suzhou Soft-Touch Robotics Technology Co., Ltd., China) integrated with our sensor to show the robot a sense of touch.

ASSOCIATED CONTENT

Supporting Information

The Supporting Information is available free of charge at <https://pubs.acs.org/doi/10.1021/acsnano.1c10535>.

Demonstration of the flexibility and resistance of the microstructured electrode in different mechanical states, stability of the microstructured electrodes, table of the comparison between our pressure sensors and other capacitive sensors in terms of sensitivity and linear sensing range, signal stability of our sensor under different relative humidity values, objects with different weights measured with a commercial electronic balance, elastic modulus of the PVA/H₃PO₄ film, elastic modulus of the epoxy resin/Au electrode (PDF)

AUTHOR INFORMATION

Corresponding Author

Chuan Fei Guo – Department of Materials Science and Engineering, Southern University of Science and Technology, Shenzhen 518055, China; orcid.org/0000-0003-4513-3117; Email: guocf@sustech.edu.cn

Authors

Ningning Bai – School of Materials Science and Engineering, Harbin Institute of Technology, Harbin 150001, China; Department of Materials Science and Engineering, Southern University of Science and Technology, Shenzhen 518055, China

Liu Wang – Department of Materials Science and Engineering, Southern University of Science and Technology, Shenzhen 518055, China

Yiheng Xue – Department of Computer Science and Engineering, Southern University of Science and Technology, Shenzhen 518055, China

Yan Wang – Department of Physics, Nanchang University, Nanchang 330031, China

Xingyu Hou – Department of Materials Science and Engineering, Southern University of Science and Technology, Shenzhen 518055, China

Gang Li – Department of Materials Science and Engineering, Southern University of Science and Technology, Shenzhen 518055, China

Yuan Zhang – Department of Materials Science and Engineering, Southern University of Science and Technology, Shenzhen 518055, China

Minkun Cai – Department of Materials Science and Engineering, Southern University of Science and Technology, Shenzhen 518055, China

Lingyu Zhao – Department of Materials Science and Engineering, Southern University of Science and Technology, Shenzhen 518055, China

Fangyi Guan – Department of Materials Science and Engineering, Southern University of Science and Technology, Shenzhen 518055, China

Xueyong Wei – State key Laboratory for Manufacturing Systems Engineering, Xi'an Jiaotong University, Xi'an, Shaanxi 710049, China; orcid.org/0000-0002-6443-4727

Complete contact information is available at:
<https://pubs.acs.org/10.1021/acsnano.1c10535>

Author Contributions

C.F.G. conceived ideas and polished the manuscript. N.N.B. conceived ideas and conducted the majority of experiments. L.W. performed the FEA simulation. Y.H.X. performed the machine learning. All authors discussed the results and have given approval to the final version of the manuscript.

Notes

The authors declare no competing financial interest.

ACKNOWLEDGMENTS

The work was supported by the National Natural Science Foundation of China (No. 52073138), the “Science Technology and Innovation Committee of Shenzhen Municipality” (Grant Nos. JCYJ20170817111714314 and JCYJ20210324120202007), the “Guangdong Innovative and Entrepreneurial Research Team Program” under Contract No. 2016ZT06G587, the Shenzhen Sci-Tech Fund (No. KYTDPT20181011104007), the “Guangdong Provincial Key Laboratory Program” (No. 2021B1212040001), and the Centers for Mechanical Engineering Research and Education at MIT and SUSTech.

REFERENCES

- (1) Chortos, A.; Bao, Z. Skin-Inspired Electronic Devices. *Mater. Today* **2014**, *17*, 321–331.
- (2) Boutry, C. M.; Negre, M.; Jorda, M.; Vardoulis, O.; Chortos, A.; Khatib, O.; Bao, Z. A Hierarchically Patterned, Bioinspired E-skin Able to Detect the Direction of Applied Pressure for Robotics. *Sci. Robot.* **2018**, *3*, No. eaau6914.
- (3) Sundaram, S.; Kellnhofer, P.; Li, Y.; Zhu, J. Y.; Torralba, A.; Matusik, W. Learning the Signatures of the Human Grasp Using a Scalable Tactile Glove. *Nature* **2019**, *569*, 698–702.
- (4) Yang, J.; Liu, Q.; Deng, Z.; Gong, M.; Lei, F.; Zhang, J.; Zhang, X.; Wang, Q.; Liu, Y.; Wu, Z.; Guo, C. F. Ionic Liquid-Activated Wearable Electronics. *Mater. Today Phys.* **2019**, *8*, 78–85.
- (5) Yang, J. C.; Mun, J.; Kwon, S. Y.; Park, S.; Bao, Z.; Park, S. Electronic Skin: Recent Progress and Future Prospects for Skin-Attachable Devices for Health Monitoring, Robotics, and Prosthetics. *Adv. Mater.* **2019**, *31*, 1904765.
- (6) Li, X.; Fan, Y. J.; Li, H. Y.; Cao, J. W.; Xiao, Y. C.; Wang, Y.; Liang, F.; Wang, H. L.; Jiang, Y.; Wang, Z. L.; Zhu, G. Ultracomfortable Hierarchical Nanonetwork for Highly Sensitive Pressure Sensor. *ACS Nano* **2020**, *14*, 9605–9612.
- (7) Huang, Y.; Fan, X.; Chen, S. C.; Zhao, N. Emerging Technologies of Flexible Pressure Sensors: Materials, Modeling, Devices, and Manufacturing. *Adv. Funct. Mater.* **2019**, *29*, 1808509.
- (8) Gu, G.; Zhang, N.; Xu, H.; Lin, S.; Yu, Y.; Chai, G.; Ge, L.; Yang, H.; Shao, Q.; Sheng, X.; et al. A Soft Neuroprosthetic Hand Providing Simultaneous Myoelectric Control and Tactile Feedback. *Nat. Biomed. Eng.* **2021**, 1–10.
- (9) Yin, R. Y.; Wang, D. P.; Zhao, S. F.; Lou, Z.; Shen, G. Z. Wearable Sensors-Enabled Human-Machine Interaction Systems: From Design to Application. *Adv. Funct. Mater.* **2021**, *31*, 2008936.
- (10) Chen, L.; Lu, M.; Yang, H.; Salas Avila, J. R.; Shi, B.; Ren, L.; Wei, G.; Liu, X.; Yin, W. Textile-Based Capacitive Sensor for Physical Rehabilitation via Surface Topological Modification. *ACS Nano* **2020**, *14*, 8191–8201.
- (11) Chhetry, A.; Kim, J.; Yoon, H.; Park, J. Y. Ultrasensitive Interfacial Capacitive Pressure Sensor Based on a Randomly Distributed Microstructured Iontronic Film for Wearable Applications. *ACS Appl. Mater. Interfaces* **2019**, *11*, 3438–3449.
- (12) Li, T.; Luo, H.; Qin, L.; Wang, X.; Xiong, Z.; Ding, H.; Gu, Y.; Liu, Z.; Zhang, T. Flexible Capacitive Tactile Sensor Based on Micropatterned Dielectric Layer. *Small* **2016**, *12*, 5042–5048.
- (13) Wan, Y.; Qiu, Z.; Huang, J.; Yang, J.; Wang, Q.; Lu, P.; Yang, J. L.; Zhang, J.; Huang, S.; Wu, Z.; Guo, C. F. Natural Plant Materials as Dielectric Layer for Highly Sensitive Flexible Electronic Skin. *Small* **2018**, *14*, 1801657.
- (14) Qiu, Z.; Wan, Y.; Zhou, W.; Yang, J.; Huang, J.; Zhang, J.; Liu, Q.; Huang, S.; Bai, N.; et al. Ionic Skin with Biomimetic Dielectric Layer Templated From Calathea Zebrine Leaf. *Adv. Funct. Mater.* **2018**, *28*, 1802343.
- (15) Mannsfeld, S. C.; Tee, B. C.; Stoltenberg, R. M.; Chen, C. V. H.; Barman, S.; Muir, B. V.; Sokolov, A. N.; Reese, C.; Bao, Z. Highly Sensitive Flexible Pressure Sensors with Microstructured Rubber Dielectric Layers. *Nat. Mater.* **2010**, *9*, 859–864.
- (16) Zhang, Z.; Gui, X.; Hu, Q.; Yang, L.; Yang, R.; Huang, B.; Yang, B.-R.; Tang, Z. Highly Sensitive Capacitive Pressure Sensor Based on a Micropyramid Array for Health and Motion Monitoring. *Adv. Electron. Mater.* **2021**, *7*, 2100174.
- (17) Luo, Z.; Chen, J.; Zhu, Z.; Li, L.; Su, Y.; Tang, W.; Omisore, O. M.; Wang, L.; Li, H. High-Resolution and High-Sensitivity Flexible Capacitive Pressure Sensors Enhanced by a Transferable Electrode Array and a Micropillar-PVDF Film. *ACS Appl. Mater. Interfaces* **2021**, *13*, 7635–7649.
- (18) Luo, Y.; Shao, J.; Chen, S.; Chen, X.; Tian, H.; Li, X.; Wang, L.; Wang, D.; Lu, B. Flexible Capacitive Pressure Sensor Enhanced by Tilted Micropillar Arrays. *ACS Appl. Mater. Interfaces* **2019**, *11*, 17796–17803.
- (19) Wu, J.; Yao, Y.; Zhang, Y.; Shao, T.; Wu, H.; Liu, S.; Li, Z.; Wu, L. Rational Design of Flexible Capacitive Sensors with Highly Linear Response over a Broad Pressure Sensing Range. *Nanoscale* **2020**, *12*, 21198–21206.
- (20) Yoo, D.; Won, D. J.; Cho, W.; Lim, J.; Kim, J. Double Side Electromagnetic Interference-Shielded Bending-Insensitive Capacitive-Type Flexible Touch Sensor with Linear Response over a Wide Detection Range. *Adv. Mater. Technol.* **2021**, *6*, 2100358.
- (21) Yang, J.; Tang, D.; Ao, J.; Ghosh, T.; Neumann, T. V.; Zhang, D.; Piskarev, Y.; Yu, T.; Truong, V. K.; Xie, K.; Lai, Y.; Li, Y.; Dickey, M. D. Ultrasoft Liquid Metal Elastomer Foams with Positive and Negative Piezopermittivity for Tactile Sensing. *Adv. Funct. Mater.* **2020**, *30*, 2002611.
- (22) Ha, K. H.; Zhang, W.; Jang, H.; Kang, S.; Wang, L.; Tan, P.; Hwang, H.; Lu, N. Highly Sensitive Capacitive Pressure Sensors over a Wide Pressure Range Enabled by the Hybrid Responses of a Highly Porous Nanocomposite. *Adv. Mater.* **2021**, *33*, 2103320.
- (23) Nie, B. Q.; Li, R. Y.; Brandt, J. D.; Pan, T. R. Iontronic Microdroplet Array for Flexible Ultrasensitive Tactile Sensing. *Lab Chip* **2014**, *14*, 1107–1116.
- (24) Cho, S. H.; Lee, S. W.; Yu, S.; Kim, H.; Chang, S.; Kang, D.; Hwang, I.; Kang, H. S.; Jeong, B.; Kim, E. H.; Cho, S. M.; Kim, K. L.; Lee, H.; Shim, W.; Park, C. Micropatterned Pyramidal Ionic Gels for

Sensing Broad-Range Pressures with High Sensitivity. *ACS Appl. Mater. Interfaces* **2017**, *9*, 10128–10135.

(25) Lei, Z.; Wang, Q.; Sun, S.; Zhu, W.; Wu, P. A Bioinspired Mineral Hydrogel as a Self-Healable, Mechanically Adaptable Ionic Skin for Highly Sensitive Pressure Sensing. *Adv. Mater.* **2017**, *29*, 1700321.

(26) Chang, Y.; Wang, L.; Li, R.; Zhang, Z.; Wang, Q.; Yang, J.; Guo, C. F.; Pan, T. First Decade of Interfacial Iontronic Sensing: From Droplet Sensors to Artificial Skins. *Adv. Mater.* **2021**, *33*, 2003464.

(27) Nie, B. Q.; Li, R. Y.; Cao, J.; Brandt, J. D.; Pan, T. R. Flexible Transparent Iontronic Film for Interfacial Capacitive Pressure Sensing. *Adv. Mater.* **2015**, *27*, 6055–6062.

(28) Bai, N.; Wang, L.; Wang, Q.; Deng, J.; Wang, Y.; Lu, P.; Huang, J.; Li, G.; Zhang, Y.; Yang, J.; Xie, K.; Zhao, X.; Guo, C. F. Graded Intrafillable Architecture-Based Iontronic Pressure Sensor with Ultra-Broad-Range High Sensitivity. *Nat. Commun.* **2020**, *11*, 1–9.

(29) Lu, P.; Wang, L.; Zhu, P.; Huang, J.; Wang, Y.; Bai, N.; Wang, Y.; Li, G.; Yang, J.; Xie, K.; Zhang, J.; Yu, B.; Dai, Y.; Guo, C. F. Iontronic Pressure Sensor with High Sensitivity and Linear Response over a Wide Pressure Range Based on Soft Micropillared Electrodes. *Sci. Bull.* **2021**, *66*, 1091–1100.

(30) Xiao, Y.; Duan, Y.; Li, N.; Wu, L.; Meng, B.; Tan, F.; Lou, Y.; Wang, H.; Zhang, W.; Peng, Z. Multilayer Double-Sided Microstructured Flexible Iontronic Pressure Sensor with a Record-Wide Linear Working Range. *ACS Sensors* **2021**, *6*, 1785–1795.

(31) Choi, W.; Lee, J.; Kyoung Yoo, Y.; Kang, S.; Kim, J.; Hoon Lee, J. Enhanced Sensitivity of Piezoelectric Pressure Sensor with Microstructured Polydimethylsiloxane Layer. *Appl. Phys. Lett.* **2014**, *104*, 123701.

(32) Zhang, Y.; Han, F.; Hu, Y.; Xiong, Y.; Gu, H.; Zhang, G.; Zhu, P.; Sun, R.; Wong, C. P. Flexible and Highly Sensitive Pressure Sensors with Surface Discrete Microdomes Made from Self-Assembled Polymer Microspheres Array. *Macromol. Chem. Phys.* **2020**, *221*, 2000073.

(33) Borok, A.; Laboda, K.; Bonyar, A. PDMS Bonding Technologies for Microfluidic Applications: A Review. *Biosensors* **2021**, *11*, 292.

(34) Semoto, T.; Tsuji, Y.; Yoshizawa, K. Molecular Understanding of the Adhesive Force between a Metal Oxide Surface and an Epoxy Resin. *J. Phys. Chem. C* **2011**, *115*, 11701–11708.

(35) Zhang, Y.; Hasegawa, K.; Kamo, S.; Takagi, K.; Ma, W.; Takahara, A. Enhanced Adhesion Effect of Epoxy Resin on Metal Surfaces Using Polymer with Catechol and Epoxy Groups. *ACS Appl. Polym. Mater.* **2020**, *2*, 1500–1507.

(36) Shao, R.; Wang, C.; Wang, G.; Zhao, J.; Sun, S. A Highly Accurate, Stretchable Touchpad for Robust, Linear, and Stable Tactile Feedback. *Adv. Mater. Technol.* **2020**, *5*, 1900864.

(37) Qin, H.; Owyung, R. E.; Sonkusale, S. R.; Panzer, M. J. Highly Stretchable and Nonvolatile Gelatin-Supported Deep Eutectic Solvent Gel Electrolyte-Based Ionic Skins for Strain and Pressure Sensing. *J. Mater. Chem. C* **2019**, *7*, 601–608.

(38) Choi, H. B.; Oh, J.; Kim, Y.; Pyatykh, M.; Chang Yang, J.; Ryu, S.; Park, S. Transparent Pressure Sensor with High Linearity over a Wide Pressure Range for 3D Touch Screen Applications. *ACS Appl. Mater. Interfaces* **2020**, *12*, 16691–16699.

(39) Ji, B.; Zhou, Q.; Lei, M.; Ding, S.; Song, Q.; Gao, Y.; Li, S.; Xu, Y.; Zhou, Y.; Zhou, B. Gradient Architecture-Enabled Capacitive Tactile Sensor with High Sensitivity and Ultrabroad Linearity Range. *Small* **2021**, *17*, 2103312.

(40) Zheng, Y.; Lin, T.; Zhao, N.; Huang, C.; Chen, W.; Xue, G.; Wang, Y.; Teng, C.; Wang, X.; Zhou, D. Highly Sensitive Electronic Skin with a Linear Response Based on the Strategy of Controlling the Contact Area. *Nano Energy* **2021**, *85*, 106013.

(41) Sundaram, S.; Kellnhofer, P.; Li, Y.; Zhu, J. -Y.; Torralba, A.; Matusik, W. Learning the Signatures of the Human Grasp Using a Scalable Tactile Glove. *Nature* **2019**, *569*, 698–702.

(42) Jin, T.; Sun, Z.; Li, L.; Zhang, Q.; Zhu, M.; Zhang, Z.; Yuan, G.; Chen, T.; Tian, Y.; Hou, X.; Lee, C. Triboelectric Nanogenerator

Sensors for Soft Robotics Aiming at Digital Twin Applications. *Nat. Commun.* **2020**, *11*, 1–12.

Recommended by ACS

Highly Stretchable and Sensitive Pressure Sensor Array Based on Icicle-Shaped Liquid Metal Film Electrodes

Yiqiu Zhang, Jian Liu, *et al.*

JUNE 05, 2020
ACS APPLIED MATERIALS & INTERFACES

READ 

Multilayer Double-Sided Microstructured Flexible Iontronic Pressure Sensor with a Record-wide Linear Working Range

Yan Xiao, Zhengchun Peng, *et al.*

MAY 05, 2021
ACS SENSORS

READ 

Highly Sensitive Membrane-Based Pressure Sensors (MePS) for Real-Time Monitoring of Catalytic Reactions

Alessandra Zizzari, Valentina Arima, *et al.*

MAY 16, 2018
ANALYTICAL CHEMISTRY

READ 

Three-Dimensional Printing of a Flexible Capacitive Pressure Sensor Array in the Assembly Network of Carbon Fiber Electrodes and Interlayer of a Porous P...

Ruiqing Li, Xueliang Xiao, *et al.*

SEPTEMBER 03, 2021
ACS APPLIED ELECTRONIC MATERIALS

READ 

Get More Suggestions >